# Improved detection of airborne volcanic ash using multispectral infrared satellite data

Gary P. Ellrod

Office of Research and Applications, National Environmental Satellite Data and Information Service, National Oceanic and Atmospheric Administration, Camp Springs, Maryland, USA

Bernadette H. Connell

Cooperative Institute for Research in the Atmosphere, Colorado State University, Fort Collins, Colorado, USA

Donald W. Hillger

Regional and Mesoscale Meteorology Team, National Environmental Satellite Data and Information Service, National Oceanic and Atmospheric Administration, Fort Collins, Colorado, USA

Received 26 July 2002; revised 20 December 2002; accepted 10 March 2003; published 21 June 2003.

[1] A technique for improved detection of airborne volcanic ash has been developed that uses three infrared (IR) bands from meteorological satellites. The three IR bands are centered near 3.9, 10.7, and 12.0 μm wavelength. The technique is based on the sum of two brightness temperature differences (BTDs), scaled to maximize the brightness and contrast of volcanic ash in the output image. The physical effects attributed to the observed BTDs that help distinguish the volcanic ash from various meteorological cloud types are (1) differential absorption by volcanic ash or sulfur dioxide at 3.9 μm, 10.7 μm, and 12.0 μm and (2) strong solar reflectance by ash at 3.9 μm, which varies diurnally. On the basis of two examples using data from the Geostationary Operational Environmental Satellite (GOES) the three-band IR technique is shown to provide better discrimination of volcanic ash from meteorological clouds than is possible using existing two-band methods. This conclusion is supported by comparisons of brightness count profiles and estimation of false ash detection rate statistics. The best results from the three-band IR technique are obtained during daylight hours over any surface, and at night when the ash cloud is over the ocean or other large body of water. The three-band IR technique is one of the tools currently being employed operationally at the Washington Volcanic Ash Advisory Center. *INDEX TERMS:* 0305 Atmospheric Composition and Structure: Aerosols and particles (0345, 4801); 0370 Atmospheric Composition and Structure: Volcanic effects (8409); 0394 Atmospheric Composition and Structure: Instruments and techniques; 3360 Meteorology and Atmospheric Dynamics: Remote sensing; 8419 Volcanology: Eruption monitoring (7280); *KEYWORDS:* volcanoes, volcanic ash, aviation hazards, volcanic hazards, remote sensing, volcanic clouds

**Citation:** Ellrod, G. P., B. H. Connell, and D. W. Hillger, Improved detection of airborne volcanic ash using multispectral infrared satellite data, *J. Geophys. Res.*, *108*(D12), 4356, doi:10.1029/2002JD002802, 2003.

## 1. Introduction

[2] Volcanic ash poses a potentially serious hazard to high-altitude jet aircraft along major air routes adjacent to active volcanoes. Ash clouds may persist for many hours, or perhaps days, and have been known to produce en route flight diversions in regions thousands of kilometers from their source. While no fatalities have occurred yet, there have been a number of near catastrophes involving inadvertent encounters of jet aircraft with ash clouds [*Miller and Casadevall*, 2000]. In 1997, the World Meteorological Organization established a system of Volcanic Ash Advisory Centers (VAAC), who are responsible for issuing operational advisories on current and forecast locations of airborne ash clouds within their assigned areas, day and night.

[3] Because of the isolated locations of many volcanoes, remote sensing plays an important role in tracking ash clouds as they drift away from an erupting volcano. Remote sensing techniques attempt to distinguish the ash from meteorological clouds and the underlying surfaces both day and night. Frequent, high-resolution coverage is desirable in order to track ash plumes in a timely manner. Meteorological satellites, though not originally designed for this purpose, have become valuable tools for determining the location and movement of volcanic ash. *Oppenheimer* [1998] summarizes remote sensing techniques used in the monitoring of volcanic hazards since the early 1980s. Both daytime visible, and day-night infrared (IR) sensors


0148-0227/03/2002JD002802

are provided by geostationary satellites at moderately high spatial resolutions (1–5 km) and frequency (15 min–1 hr). Although daylight visible imagery is used extensively, it cannot readily distinguish the ash cloud from certain types of meteorological clouds and aerosols, except possibly for explosive eruptions that are very low in water content. Identification of volcanic ash relies mostly on differences in radiative properties between the ash cloud and adjacent meteorological clouds observed in IR satellite imagery [*Oppenheimer*, 1998].

[4] A bi-spectral image technique for the detection of volcanic ash, derived from either geostationary or polar orbiting satellite data, has been used for over a decade by both operational and research meteorologists. This technique was first applied using IR data from the Advanced Very High Resolution Radiometer (AVHRR) on polar orbiting National Oceanic and Atmospheric Administration (NOAA) spacecraft. The technique is based on the observed brightness temperature difference (BTD) between the "split window" IR band centered near 12 μm wavelength (band 5 on AVHRR), and the IR window at 11 μm (band 4) [*Prata*, 1989; *Holasek and Rose*, 1991; *Schneider et al.*, 1995] to discriminate between volcanic ash clouds and meteorological clouds. A negative band 4–5 difference of $<-1^{\circ}$K is normally used as a threshold to denote the presence of ash. The physical process that leads to this effect was termed "reverse absorption" by *Prata* [1989], caused by the larger emissivity of volcanic ash at the longer wavelength. The two-band split window technique (hereinafter referred to as TBSW) has recently employed Geostationary Operational Environmental Satellite (GOES) IR data extensively in monitoring eruptions from the Popocatepetl volcano in Mexico [*Rose and Schneider*, 1996] and Soufriere Hills volcano on the island of Montserrat in the eastern Caribbean [e.g., *Davies and Rose*, 1998; *Rose and Mayberry*, 2000].

[5] There are some situations where the TBSW technique fares poorly, however [*Simpson et al.*, 2000; *Prata et al.*, 2001]. In general, these are due to the fact that the magnitude of negative TBSW BTDs is driven by (1) the height of the eruption cloud, (2) the mass per unit area of fine ash within the cloud, and (3) the size of the ash particles (smaller particles have a stronger signal). Since all of these factors are optimized in larger eruptions, smaller eruptions are more difficult to detect [*Rose and Mayberry*, 2000].

[6] Several specific environmental conditions in which these factors are present have been observed. First, within a few hours following an eruption, the presence of copious amounts of water, ice, and large ejected particles in the volcanic cloud often results in an opaque volcanic cloud, and non-discrimination of ash. Sources of water for the eruption column can be from sub-surface ground water, glacier melt, large surface bodies of water (the ocean, lakes, etc), or entrained atmospheric water vapor. For example, the strong eruption of Soufriere Hills volcano on 26 December 1997 produced a pyroclastic flow that spread offshore, resulting in superheating of the ocean surface, and the ingestion of large amounts of water vapor into the ash column [*Mayberry et al.*, 2001]. Although an eruption cloud was clearly observed in IR satellite images, the TBSW did not provide a definitive volcanic ash signal until many hours later, beginning at the periphery of the volcanic cloud.

[7] Second, the high ambient moisture content typical of atmospheric conditions in the Tropics can mask the presence of volcanic ash, or prevent clear discrimination of the ash from meteorological clouds. Most of this water vapor is contained in the lowest 3 km of the atmosphere. This condition is especially a problem for eruptions of smaller volcanoes in the tropics, such as Soufriere Hills, that frequently emit ash and steam into the lower and middle troposphere. *Yu et al.* [2002] showed that some of these small eruptions have TBSW BTDs of +1 to +3 instead of normally observed negative values. *Simpson et al.* [2000] also found that even at northern latitudes, moisture contamination can be a significant problem. Because of water vapor absorption, the area of volcanic ash can be significantly underestimated for small eruptions. Despite their relatively low altitude, these smaller eruption clouds can be hazardous to any type of aircraft during the climb or descent phase of flight.

[8] Third, the presence of a cold background scene (snow and ice covered terrain or ocean) can negate effective use of the TBSW technique. This condition is more rare within the GOES field-of-view, but has been documented for an eruption of Mt. Spurr in Alaska [*Shannon*, 1996].

[9] An example of an instrument-related failure can occur when there is an offset between the fields-of-view for bands 4 and 5, resulting in false negative TBSW BTDs. This effect is most pronounced at large displacements from the satellite nadir, such as over Alaska when using GOES data.

[10] For these reasons, there is a need to improve the detection of volcanic ash using remotely sensed IR data. Recent work described in this paper has shown that by including data from a shortwave IR (SWIR) band, centered near 4 μm, better discrimination of ash clouds can be obtained, even within a few hours after an eruption, when the TBSW often fails. This paper describes the three-band IR technique using GOES data, discusses some of the physical processes involved, and shows examples of its utility in a variety of conditions.

## 2. Application of GOES Infrared Data

[11] The GOES satellites are currently equipped with a five channel imager (one visible, four infrared), with spectral bands listed in Table 1. The resolution of the IR bands (4 km at nadir) and temporal frequency (30 min) of GOES data is sufficient for the detection and tracking of many volcanic ash plumes. Volcanic ash clouds may consist of varying amounts of water vapor and cloud droplets, silicate particles, sulphuric acid droplets, sulphur dioxide, and other gases [*Oppenheimer*, 1998]. Sulfur dioxide ($SO_2$) gas, emitted by some volcanoes, can be monitored at ultraviolet wavelengths (300–400 nm) [*Krotkov et al.*, 1997] that are not available on GOES instruments. $SO_2$ reacts with atmospheric oxygen and water molecules to produce sulphuric acid ($H_2SO_4$) droplets. These droplets, along with silicate particles, can be detected with the longwave IR bands available on either GOES or NOAA AVHRR [e.g., *Prata*, 1989], although $H_2SO_4$ tends to mask the signal from silicate ash. Because of the height differences often found between ash and $SO_2$ clouds, however, these components often separate in conditions of vertical wind shear [e.g., *Seftor et al.*, 1997], and thus may not be spatially coincident.

**Table 1.** GOES Imager Band Characteristics

| Band | Wavelength, μm | Name | Resolution, km |
|---|---|---|---|
| 1 | 0.6 | visible | 1 |
| 2 | 3.9 | shortwave | 4 |
| 3 | 6.7 | water vapor | 8 |
| 4 | 10.7 | window | 4 |
| 5 | 12.0 | longwave | 4 |

[12] GOES IR bands 4 and 5 are longwave "window" IR bands that are transparent to upwelling thermal radiation from the Earth's surface. However, band 5 is located near a water vapor absorption region, resulting in slightly cooler brightness temperatures in band 5 than band 4 in conditions where ample low-level moisture is present (T4−T5 is positive for the TBSW). On the other hand, a "reverse absorption" effect has also been observed for airborne volcanic ash [*Prata*, 1989] and Sahara dust [*Volz*, 1973], resulting in slightly warmer brightness temperatures in band 5 than in band 4 (T4−T5 is negative). These two effects thus tend to offset each other in the tropics.

[13] The physical effects leading to the thermal signature for volcanic ash in the TBSW are the variation of radiative emissivity with wavelength, coupled with differences in the transmittance of radiant energy through the ash cloud from the Earth's surface or underlying clouds. In laboratory experiments, *Vickers and Lyon* [1967] found that the emissivity of siliceous materials has a minimum value between 8.0 and 9.7 μm, which then increases with longer wavelength, becoming a maximum around 12−13 μm. The emissivity is therefore smaller at 10.7 μm than at 12.0 μm, the IR wavelengths available on GOES. A critical requirement is the semi-transparency of volcanic ash clouds. When ash clouds are opaque from dense concentrations of large water droplets, ice crystals, and large ash particles (typically the case within a few hours following a volcanic eruption), these emissivity differences are not significant enough to be detectable.

[14] The GOES shortwave infrared (SWIR) band 2 (3.9 μm) on GOES is a window channel characterized by little or no moisture absorption, and very high sensitivity to heat sources (such as fires or volcanoes). The SWIR band also has a strong component from daytime solar reflectance as well, which can overwhelm the emitted thermal energy for some types of clouds or surface features [*Turk et al.*, 1998]. Using AVHRR imagery in the SWIR (3.55−3.93 μm) and longwave infrared (LWIR) (10.3−11.3 μm) bands for analysis of the ash cloud from 1989−1990 eruptions of Redoubt Volcano in Alaska, *Schneider and Rose* [1994] showed that the BTD between the SWIR and LWIR bands was useful for enhancing certain volcanic ash clouds, but by itself did not help to distinguish them from meteorological clouds. The reasons for this are linked to the characteristics of ash, water and ice clouds at these wavelengths. If these characteristics are better understood and accounted for, the ash signal may be detected using SWIR alone, but by combining SWIR with the existing TBSW, an even stronger ash detection signal is attainable.

[15] The SWIR-LWIR BTD (hereinafter referred to as SLIR) has been used to distinguish between low-level fog and stratus cloud from dense cirrus, high-level ice cloud, and background both during the day and at night [*Ellrod*, 1994; *Lee et al.*, 1997]. During the day, the reflectance from practically all surfaces (cloud and Earth) has the effect of increasing the brightness temperature for the SWIR until it becomes larger than the emitted LWIR component, producing a positive SLIR.

[16] Looking at cloud properties during the day with the SWIR band alone, water clouds can be distinguished from ice clouds by their reflectance. The reflectance of water clouds in the shortwave region is inversely proportional to the effective radius of the cloud particles in the 5−20 μm radius range [*Kleespies*, 1995; *Arking and Childs*, 1985], and is larger than the reflectance of ice clouds composed of similar sized particles. Reflectance of larger (20−1000 μm) ice particles has also been shown to decrease with increasing size. In summary, clouds comprised of small water droplets are more reflective than those comprised of either large water droplets or ice particles. Thus lower level eruption clouds, composed mainly of ash and water droplets, will be significantly enhanced, whereas higher altitude eruption clouds (reaching at least −40 C and composed chiefly of ice particles) will not be enhanced as much.

[17] For volcanic ash samples, the bi-conical reflectance is 20−50% higher in the 3.9 μm region than in the 10.7 or 12.0 μm region [*Schneider and Rose*, 1994]. *Salisbury and Walter* [1989] show similar relations for quartz particles in the 1−43 μm size range. This reflectance peak is dramatically shown by Figure 1 for four ash samples from an eruption of Redoubt Volcano on 8 January 1990. Comparisons from a number of eruptions showed that the magnitude of reflectance was more dependent on particle size than composition. For an ash cloud with particle sizes <20 μm, we would then expect to see a significant increase in reflectance over that observed for either water or ice cloud. This would translate to a warmer SWIR brightness temperature, and a larger (positive) SLIR. However, a cloud containing a mixture of volcanic ash, ice and water droplets may respond in a variety of ways, depending on relative proportions of each substance.

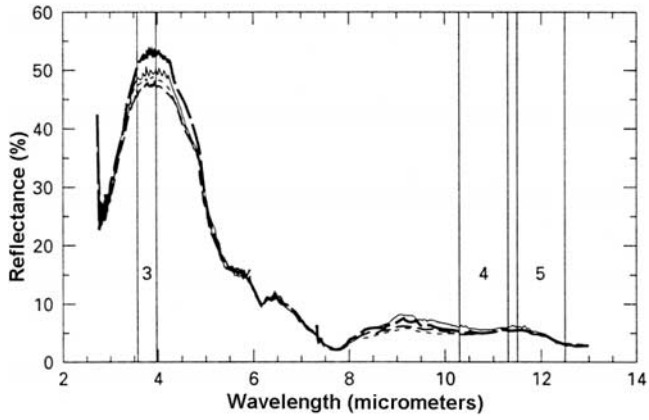


**Figure 1.** Plot of reflectance versus wavelength for four volcanic ash samples from an eruption of Redoubt Volcano on 8 January 1990. Wavelength range '3' denotes the 3.7 μm IR band on the Advanced Very High Resolution Radiometer (AVHRR), '4' is the 11.0 μm band, and '5' is the 12.0 μm band. (From *Schneider et al.* [1995].)

[18] The solar scattering by volcanic aerosols observed at 3.9 μm results in a pronounced diurnal variation through the course of the day. It is complicated by its anisotropic character so that the relative position of the Sun and the satellite sensor with respect to the ash cloud is an important factor. The result of preferential forward scattering by ash particles is that the maximum SLIR BTD values should be observed during the morning hours for ash clouds located east of the satellite sub-point and during the afternoon hours for ash clouds west of the sub-point.

[19] At night, there is little or no reflective component, so the emissivity and transmittance characteristics of the ash particles become dominant. Emissivity, which is often difficult to measure, must satisfy the relationship:

$$\rho + \tau + \epsilon = 1 \tag{1}$$

where $\rho$ is reflectivity, $\tau$ is transmissivity, and $\epsilon$ is emissivity. In the simple case of an opaque cloud or other object, $\tau$ becomes zero. For water cloud, emissivity is lower in the 3.9 μm region than in the 10.7 μm region, which results in a negative SLIR at night. With ice cloud, the same pattern is seen, but the magnitude of the emissivity difference is much smaller. Transmissivity at 3.9 μm is greater than at 10.7 μm, particularly for cirrus, in which the population of cloud particles is less than in a water cloud and also because the cirrus clouds tend to be vertically thinner than water clouds [*Kidder and Vonder Haar*, 1995].

[20] Two patterns are normally observed for cirrus clouds with the SLIR at night: (1) a positive BTD, and (2) an "out-of-range" signal in which rapid, extreme variations in BTD occur. The first pattern results from the assumption of negligible transmission being incorrect. *Hunt* [1973] showed that transmissivity is greater for both water and ice at 3.9 μm than at 10.7 μm when the cloud is not opaque. In the case of thin cirrus cloud for example, radiation from the background becomes important, and the 3.9 μm band temperature becomes warmer than the temperature at 10.7 μm, resulting in a positive SLIR. When the cirrus or convective (ice) cloud is opaque, the temperatures are approaching −30 to −40 C where instrument noise for the 3.9 μm band becomes large, an out-of-range signal is produced.

[21] Using relationship (1) with the results of *Schneider and Rose* [1994] and *Salisbury and Walter* [1989] for reflectivity and assuming an opaque surface ($\tau = 0$), ash at night has a lower emissivity in the 3.9 μm region than in the 10.7 μm region. However, observations reveal that SLIR is often positive for ash, so transmissivity is therefore suspected to play a significant role in producing the observed BTDs at night. There is also evidence of absorption by $SO_2$ in the SWIR [*Bishop et al.*, 1995], although the peak occurs at slightly longer wavelengths than GOES band 2 (around 4.4 μm). The resultant increase in thermal emission would enhance the positive SLIR BTD both day and night, assuming the $SO_2$ and ash clouds are juxtaposed. The only times a negative BTD is observed is when an ash plume is over a cold (snow-covered) surface where a low-level inversion is likely present. For example, *Watkin et al.* [2000] found a large negative SLIR (<−10 C) at night for an ash plume from Grimsvoten volcano in Iceland on 18 December 1988 using equivalent channels from the NOAA AVHRR.

[22] *Ackerman* [1989] found variable results in SLIR BTDs at night in his modeling analysis of dust clouds, which often consist partially of silicate minerals. SLIR values of 0 to +10 C were determined over a warm ocean surface at night depending on turbidity, but negative values were obtained over a desert scene, similar to what would be observed with certain meteorological clouds. Although the composition may be somewhat different, we may conclude from this that volcanic ash detection at night is likely to be better from SLIR data over warm oceans than over land. During the daytime, SLIR was strongly positive for both types of scenes, but larger over a desert than over an ocean surface.

[23] Beside the aspect of transmissivity, the limitations of the 3.9 μm band for measurements in cold scenes become dominant. Because of the steep slope of the Planck function at cold temperatures (<−40 C), the instrument noise at 3.9 μm becomes very large [*Hillger*, 1999]. The sensors also reach saturation at −68 C. For these reasons, the 3.9 μm data should not be used for temperatures colder than −40 C (233 K) and are not currently used in operational versions of the experimental product described in the next section.

[24] In summary, the contribution of the 3.9 μm band in volcanic ash detection is primarily from: (1) enhanced solar reflectance during the daylight hours resulting in large, positive SLIR BTDs, and (2) differential absorption and transmittance at night, resulting in smaller positive BTDs that are still relatively larger than those of cloud and surface features, with the best results over warm oceans, and (3) absorption by $SO_2$ either day or night. Large negative SLIR BTD values with volcanic ash plumes have only been observed at night when the plume overlies a cold, snow-covered surface.

[25] Definitive values for emissivity, transmittance, and reflectance for ash, water, and ice clouds are difficult to obtain. The main point is that we expect to see a complex variety of BTD patterns between ash, water, and ice clouds based on what is known about the emissivity and reflectivity of each. The TBSW and SLIR often tend to complement each other such that the likelihood of detecting volcanic ash is higher with the combined use of the two than with either component alone. The addition of the SWIR band also provides additional information to help distinguish volcanic ash from meteorological clouds. In section 6, examples will show that the ash signal obtained from three IR bands is an improvement over that from only one or two bands.

## 3. Product Generation and Display

[26] In order to best utilize the properties described above, a three-band volcanic ash product (TVAP) is generated by adding the SLIR to an enhanced TBSW image. The experimental volcanic ash product can thus be described simply as:

$$B = C + m_1(T_5 - T_4) + m_2(T_2 - T_4) \tag{2}$$

TBSW SLIR

where B is output brightness temperature (K), C is a constant, $m_1$ and $m_2$ are scaling factors, and $T_2$, $T_4$, $T_5$ are

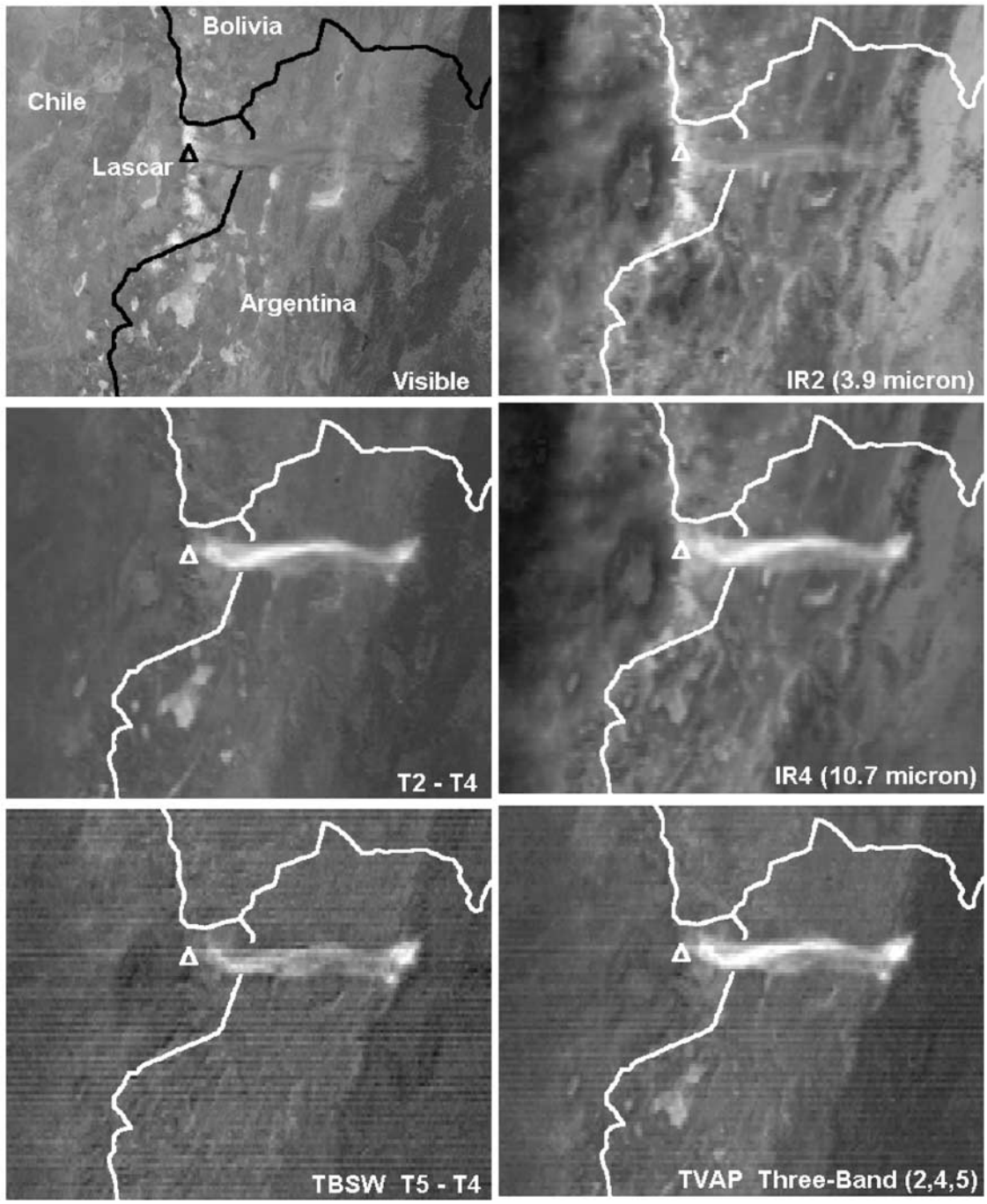


**Figure 2.** GOES-8 images at 1639 UTC, 20 July 2000 for: the visible band (upper left), IR band 2 (3.9 μm) (top right), IR bands 2–4 (middle left), IR window band 4 (10.7 μm) (middle right), two-band split window (TBSW) (5–4) (lower left), and the three-band volcanic ash product (TVAP) (lower right).

the brightness temperatures (K) for bands 2, 4 and 5, respectively. The $T_5$ - $T_4$ difference is used here for the TBSW instead of the usual convention, since the former typically results in a positive value for volcanic ash. The values for C and m were originally determined empirically to produce optimum contrast based on observed volcanic eruptions. Later adjustments were made to those parameters by means of principal component analysis (PCA) techniques, which are described in the next section. The values currently in use for C, $m_1$, and $m_2$ are 60, 10, and 3, respectively. Thus the TBSW term has about three times the contribution to the TVAP image than does the SLIR term. In situations where volcanic ash is present, both TBSW and SLIR terms are maximized (particularly during daylight hours), and the value of B approaches 255, the maximum count value for 8-bit video displays. However, because of the complexity of radiative processes at 3.9 μm wavelength described in the previous section, especially during daylight hours, specific thresholds of B that distinguish volcanic ash from non-ash features have not been established. Rather, it is the relative value of B within an ash cloud compared to its surroundings that allows detection and discrimination.

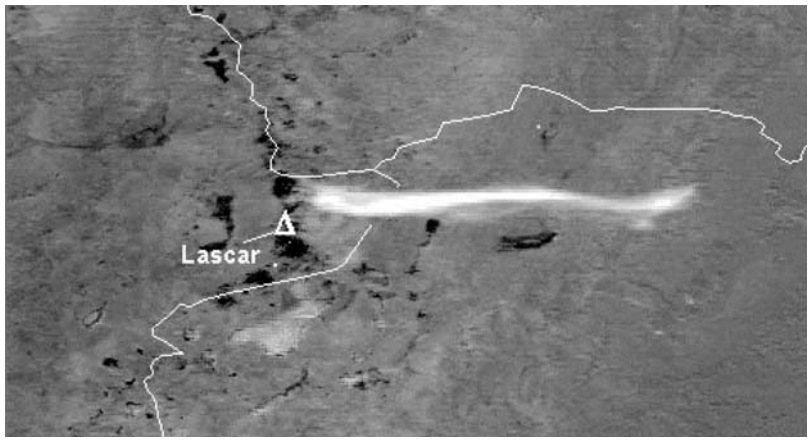


**Figure 3.** A principal component analysis (PCA) image based on five GOES-8 bands (including 0.6 μm visible band) at 1639 UTC, 20 July 2000.

Minium values of B can be as low as 60–100 at night for very thin ash clouds at night, to 200–255 for relatively thick ash clouds during daylight hours.

[27] As an alternative approach, the SLIR can also be based on reflectance, rather than BTD. The "reflectivity product" is obtained by using the $T_4$ value to solve for the emitted Planck radiance at 3.9 μm [e.g., *Allen et al.*, 1990], which is then removed from the total 3.9 μm radiance, resulting in reflectance. With no thermal component, there is usually a significant difference in reflectivity between volcanic ash and other features that results in improved detection of the ash, with the maximum difference observed during daylight hours.

## 4. Validation

[28] To show the effectiveness of the TVAP versus the well-known TBSW technique, transects of brightness value were obtained across regions of suspected volcanic ash in both types of image products for each example. Brightness information for the surrounding background surface or meteorological clouds was also obtained to show relative contrast of the ash plume with its surroundings.

[29] In addition, a quantitative estimate of the ability of each product to screen out non-volcanic ash features (clouds and surface) was obtained by image enhancement and statistical analysis of digital brightness data. Each image (TVAP and TBSW) was interactively enhanced until a brightness count range was obtained that displayed optimum area of the volcanic cloud. Animation of the 30-min interval GOES imagery from the initial eruption time was helpful in defining the "true" extent of the ash cloud. Statistical analysis was then performed to estimate the optimum area (A) (in pixels) of the volcanic cloud. Then the entire image was analyzed to determine the total number of pixels (T) within the same brightness range as the ash cloud. The "false pixel rate (FPR)" expressed in per cent of the total image area is defined as:

$$\mathrm{FPR} = 100((\mathrm{T} - \mathrm{A})/\mathrm{N}) \quad (3)$$

where N is the total number of pixels in the displayed image. To show improvement over the TBSW image, the TVAP must provide better contrast, with no significant increase in FPR.

## 5. Principal Component Analysis (PCA)

[30] Complementary work has involved the use of Principle Component Analysis (PCA), a form of eigenvector statistical analysis, to screen GOES Imager bands for pertinent information [*Hillger and Ellrod*, 2003]. PCA images help to reduce the amount of redundant information in the various GOES bands and highlight the less obvious features on the surface and in the atmosphere. The first PCA image contains information common to all bands being screened, such as clouds. The second and subsequent PCA images contain information not explained by previous components, such as band differences. The component images are ordered such that the higher numbered images explain progressively less of the total variance between the bands. Data in each image is stretched over the full 8-bit


**Figure 4.** Operational analysis issued by the Washington VAAC showing area of volcanic ash from a Lascar eruption, valid at 1909 UTC, 20 July 2000. (Hatched area indicates volcanic ash.)

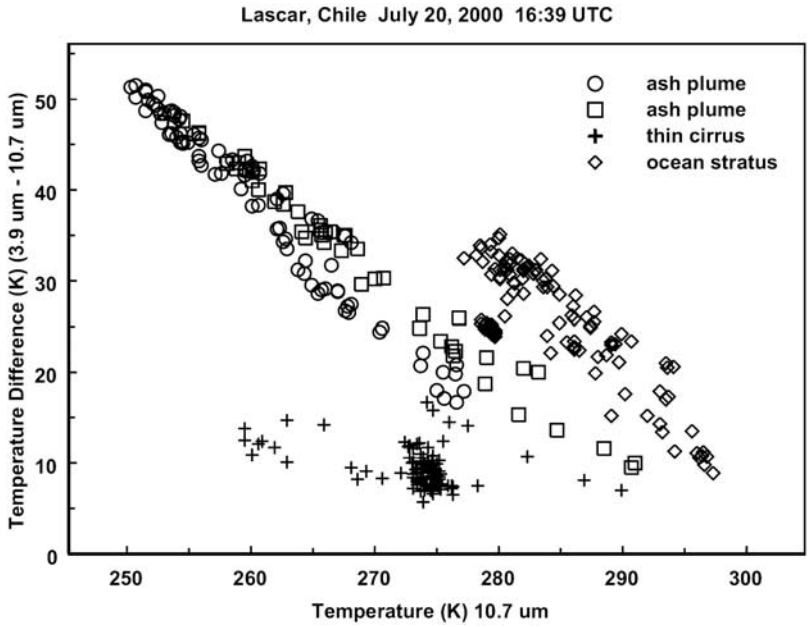


**Figure 5.** Data plot showing GOES-8 brightness temperatures (K) for IR band 4 (10.7 μm) (x-axis), and the difference between IR bands 2 (3.9 μm) and 4 (y-axis) for volcanic ash, ocean stratus and thin cirrus at 1639 UTC (Figure 2).

brightness count range to highlight the significant information. PCA techniques have been previously used in the discrimination of volcanic ash from surrounding terrain for an eruption of Mt. Redoubt in Alaska with AVHRR data [*Dean et al.*, 1994]. The relative contributions from the three bands for PCA images also provided an objective way to tune the parameters C, $m_1$ and $m_2$ in equation (1) for the TVAP. In this paper, images that utilize an independent GOES visible band (0.6 μm) will also be shown for comparison with the IR TVAP. These consist of both raw visible images and the inclusion of visible data in PCA images.

## 6. Examples

[31] Two examples of the TVAP are provided in this section to show the capability of the technique under differing atmospheric conditions and background terrain. The first example, a moderately intense eruption of Lascar volcano in northeast Chile, occurred during daytime under

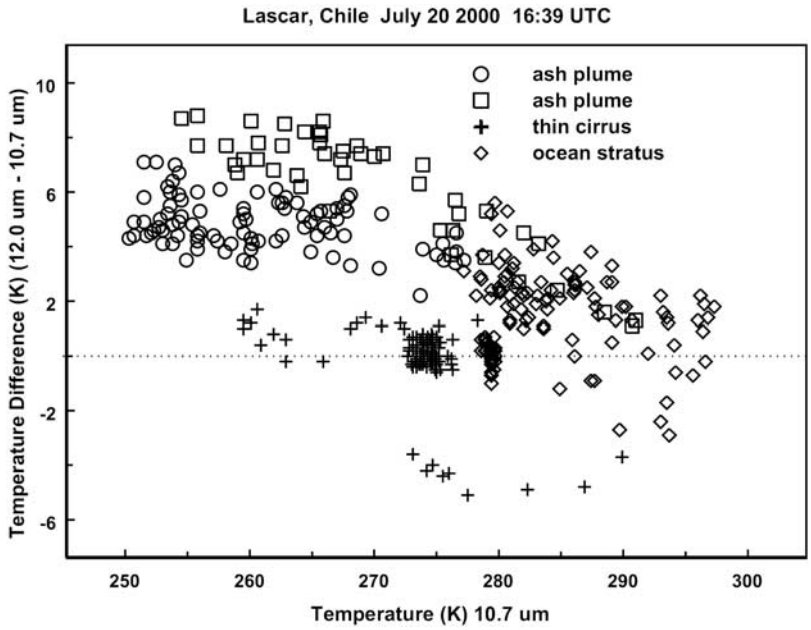


**Figure 6.** Same as Figure 5, except for IR band 4 (10.7 μm) temperature (K) (x-axis), and the temperature difference between IR bands 5 (12.0 μm) and 4 (y-axis).

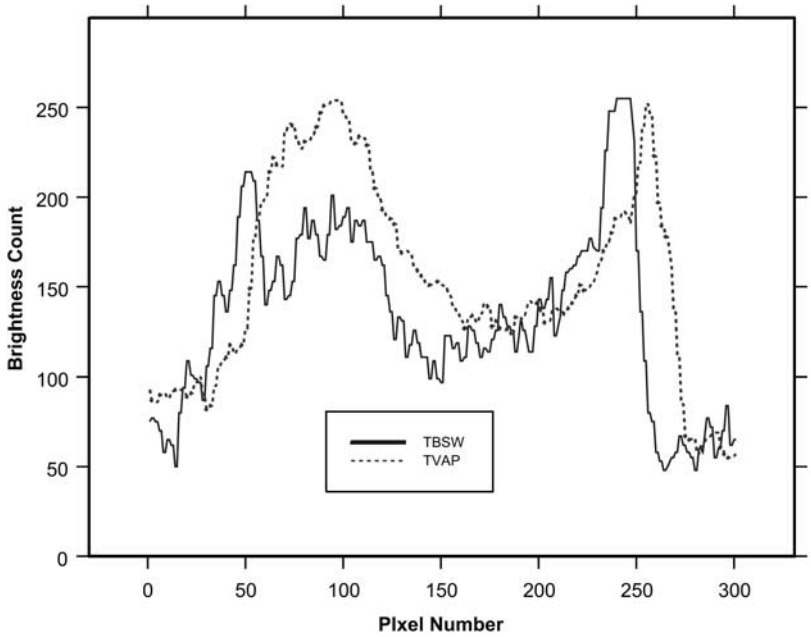


**Figure 7.** Trace of brightness count at each pixel along length of Lascar ash plume for TBSW (solid line) and TVAP (dashed line) at 1639 UTC, 20 July 2001. One pixel equals 2 km distance at this scale.

nearly cloudless conditions. The ash plume was originally located over a high desert, then drifted eastward into a more humid, vegetated low-altitude environment in Argentina. The second example, showing ash from several moderate eruptions of Soufriere Hills volcano on the island of Montserrat, occurred at night within a moist lower atmosphere and a variety of tropical cloud types in the vicinity. In both cases, the ability of single band GOES IR images is compared with both the TBSW (inverted to show negative values as light gray or white) and TVAP. While no independent satellite data is shown for validation, extrapolation of 30 min interval GOES data from the eruption time provides a reasonable estimate of eruption cloud movement and dispersal.

### 6.1. Daytime Case: Lascar, Chile

[32] On the afternoon of 20 July 2000, there was a moderate eruption of Lascar volcano in northeast Chile around 1445 UTC that sent an ash column to an altitude of more than 10.7 km (35,000 ft) (Washington Volcanic Ash Advisory Center). The resulting plume drifted rapidly eastward (at a velocity of around 120 km $h^{-1}$) across northern Argentina, and eventually to Paraguay. The six-panel image in Figure 2 shows a multispectral comparison of GOES-8 images at 1639 UTC. Shown are the band 1 visible image (upper left), band 2 IR (upper right), band 2–4 IR BTD (SLIR) (middle left), band 4 IR (middle right), band 5–4 BTD (TBSW) (lower left), and the band 2, 4, 5 TVAP (lower right). The band 5 IR image is not shown, as it appears quite similar to band 4. The absence of meteorological clouds in this area made this a simple matter to identify the ash cloud as it moved away from the volcano using animated 30 minute interval GOES images. Note that because of the bright background of the high desert terrain, the ash was rather difficult to identify in the visible image. The relatively dark appearance of the volcanic plume in the visible image suggests high ash content. The ash was also difficult to detect in the band 2 IR, because of strong reflectance that resulted in brightness temperatures similar to the background terrain, but the SLIR, TBSW, and band 4 IR images provided good discrimination of the ash cloud. However, the TVAP was superior to all of these images, when using maximum brightness contrast as a criterion.

[33] A PCA image based on data from all five GOES-8 bands, including the visible and water vapor bands, is shown in Figure 3. The area of ash coverage is shown to be nearly identical with that depicted by the three-band product. The main differences were that the PCA image had a slightly smoother appearance than the TVAP, and depicted a little more area of the thinner ash, perhaps because of the inclusion of data from the visible band. For comparison, a Washington VAAC ash cloud analysis valid at 1909 UTC (2.5 hours later) is shown in Figure 4.

[34] The SLIR and TBSW BTDs for the ash plume, thin cirrus, and stratus clouds over the adjacent East Pacific (not seen in Figure 2) are plotted in Figures 5 and 6. For both the TBSW and SLIR, the signature of the volcanic ash cloud is distinct from cirrus clouds for the band 4 IR temperatures <275 K. For band 4 IR temperatures >275 K, however, the ash signal may be confused with that of ocean stratus in the SLIR data (Figure 5).

[35] Brightness count profiles along the entire ash plume (nearly 500 km in length) for both the TVAP and TBSW image products are shown in Figure 7. The western half of the plume has larger brightness values (and better contrast) in the TVAP than in the TBSW, whereas the eastern half of the plume is similar for both images. (The ten pixel offset to the east in the TVAP profile is possibly due to enhanced solar scattering off of the eastern portion of the ash plume in the 3.9 μm band 2, as there was no significant navigational error between any of the bands). Statistical analysis

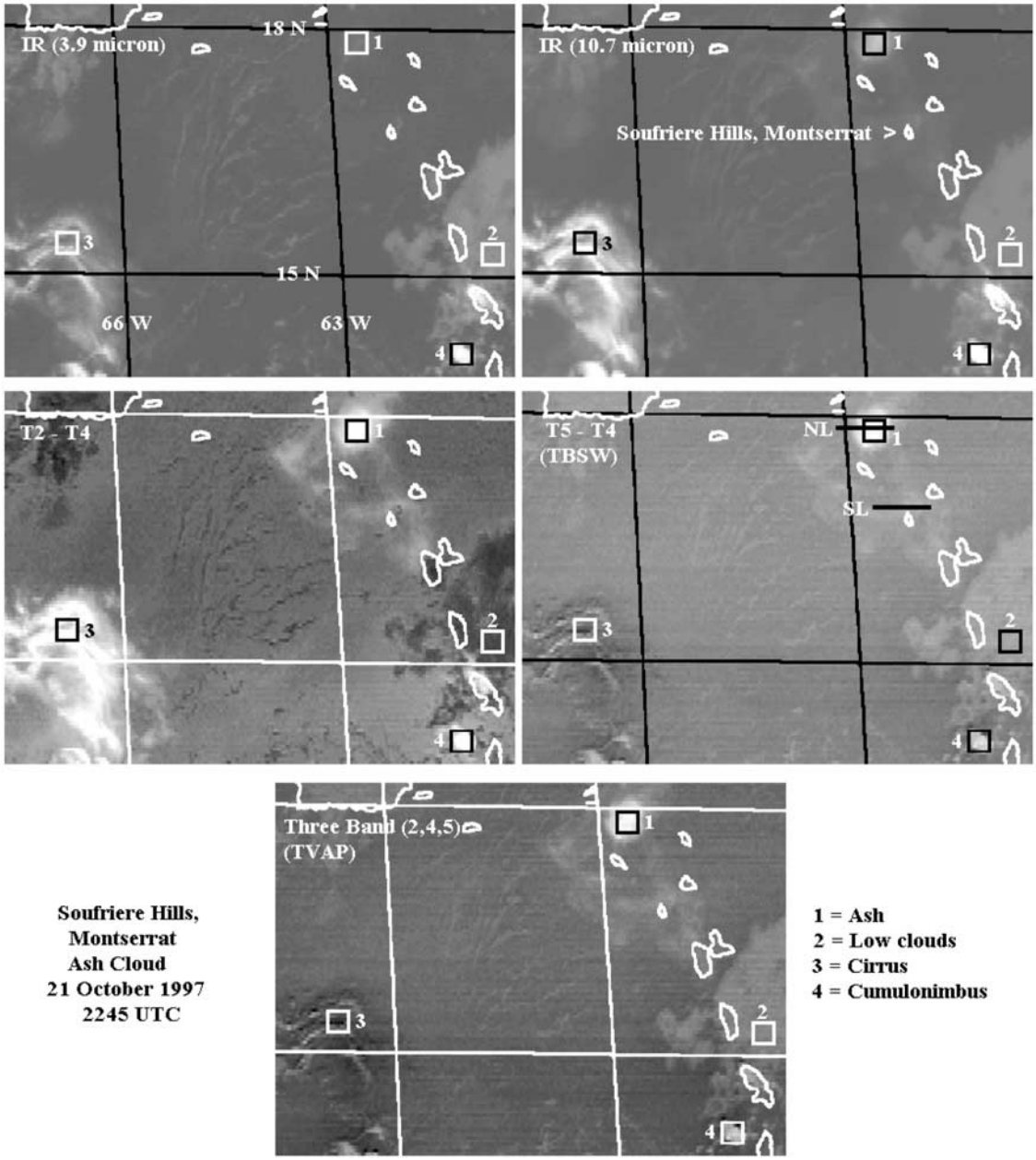


**Figure 8.** GOES-8 images showing an eruption cloud at night from the Soufriere Hills volcano on Montserrat (box 1 in top right of each panel) at 2245 UTC, 21 October 1997. Images are for IR band 2 (3.9 μm) (upper left), IR band 4 (10.7 μm) (upper right), IR bands 2–4 (middle left), IR bands 5–4 (TBSW) (middle right) and the three-band volcanic ash product (TVAP) (bottom center). Box 2 represents an area of low clouds, box 3 is cirrus, and box 4 is a cumulonimbus cloud. Lines labeled 'NL' and 'SL' in middle right panel show locations of brightness transects for northern and southern plumes in Figure 12.

of the ash cloud revealed no significant difference in the FPR values for TVAP (0.7%) versus that for TBSW (0.5%).

### 6.2. Nighttime Case: Soufriere Hills, Montserrat

[36] On 21 October 1997, an explosive eruption occurred at the Soufriere Hill, Montserrat Volcano at 1539 UTC, which quickly sent an ash column to an altitude of about 11.6 km (38,000 ft). Initially, the ash spread out in all directions, then drifted slowly to the northwest (Montserrat Volcano Observatory web page). The example presented here depicts the ash cloud characteristics seven hours after eruption, at 2245 UTC (Figure 8), and includes plotted data from an eruption plume at 2302 UTC (not shown in Figure 8). The eruption at 2302 UTC rose very quickly to between 4.6 and 6.1 km (15,000–20,000 ft) and then drifted slowly to the Northwest (Montserrat Volcano Observatory web page).

[37] Figure 8 shows GOES band 2 (3.9 μm) IR (upper left), band 4 (10.7 μm) IR (upper right), T2–T4 (SLIR), middle left), T5–T4 (TBSW) (middle right), and the three-

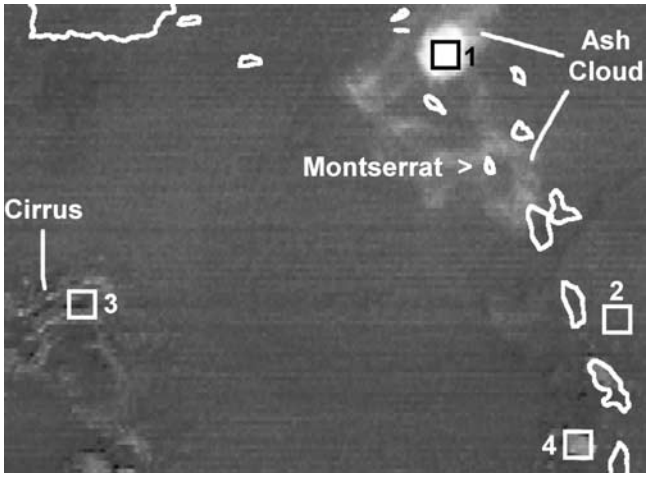


**Figure 9.** Principal component analysis (PCA) image derived from GOES-8 IR data at 2245 UTC, 21 October 1997. Boxes refer to features described in Figure 8.

band TVAP (lower center). Visible imagery is not available for this night scene. The extent of the ash cloud at this time is outlined in the TBSW image (middle right). Note that the ash cloud is difficult to detect with band 2 IR alone, an indication that transmittance is large for the plume at this wavelength. The ash cloud is more readily observed with the combined image products. The TVAP clearly distinguishes the thick portion of the ash cloud from cirrus, low cloud and an isolated deep convective cloud. Other portions of the ash cloud are not so clearly distinguished. It is assumed from this scene that the ash is not as concentrated in those regions. Although the ash cloud is difficult to distinguish completely from one image, a series of 15 minute images can be used to easily track the plume.

[38] A PCA image, based on GOES-8 IR bands 2, 4 and 5 is shown in Figure 9. This image provides good discrimination of the thick portion of the ash, and fair discrimination of the thin ash compared with the meteorological clouds. The PCA image provides slightly better depiction of the exceedingly thin portion of the ash cloud than does the TVAP (lowest panel in Figure 8).

[39] BTDs for the SLIR and TBSW for the corresponding boxed regions on Figure 8 are plotted in Figures 10 and 11. Samples were collected for the thickest portion of the ash cloud (box 1), low cloud (box 2), cirrus cloud (box 3), and a deep convective cloud (box 4). Also included is a sample of the ash taken at 0015 from an eruption at 2302 UTC. The 7-hour-old ash cloud has the characteristic positive T5–T4 (TBSW), but a convective cloud is also showing positive values. The 1-hour-old ash cloud is showing both positive and negative TBSW values. On the SLIR plot, both the 7-hour-old and the 1-hour-old ash clouds are showing a distinctive signature for warm band 4 IR temperatures, but the difference is not unique.

[40] Figure 12 shows brightness count profiles for both TVAP and TBSW across two regions of ash in Figure 8. The locations of the "northern plume" and "southern plume" are denoted in the middle right panel in Figure 8. The TVAP brightness count values are consistently larger across the region, with a significant improvement in contrast in the northern plume. Estimation of the FPR yielded values of 3.5% for TVAP versus 4.8% for TBSW, indicating that the three-band technique resulted in no degradation in quality in the remainder of the TVAP image area.

## 7. Operational Implementation and Evaluation

[41] The experimental TVAP technique was made available in February 1998 to the Washington Volcanic Ash Advisory Center (VAAC), a function of the National Envi-

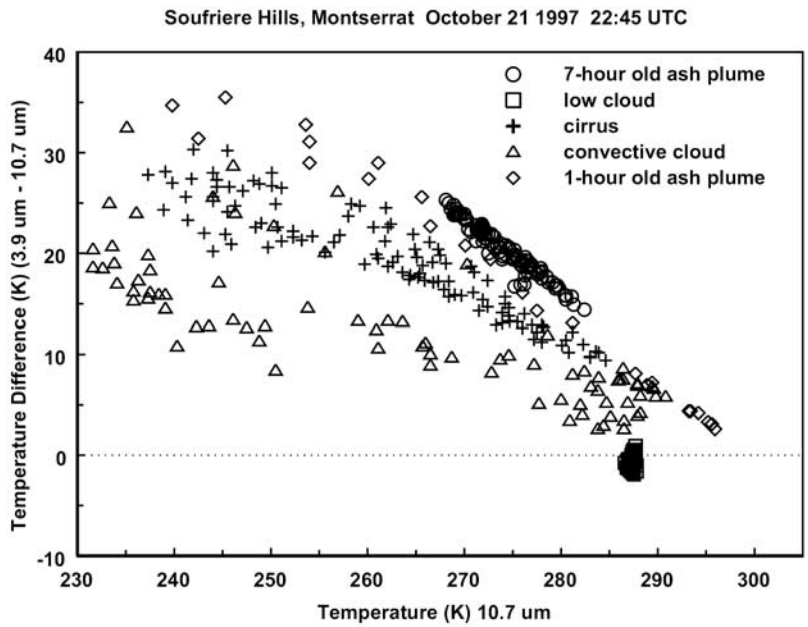


**Figure 10.** Same as Figure 5 except for the GOES-8 images at 2245 UTC on 21 October 1997.

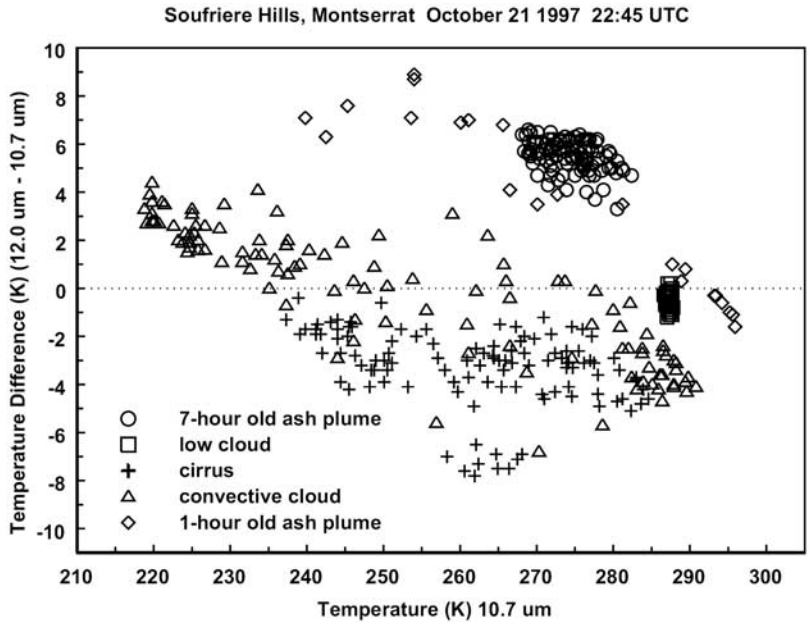


**Figure 11.** Same as Figure 6 except for the GOES-8 images at 2245 UTC on 21 October 1997.

ronmental Satellite, Data, and Information Service (NESDIS) Satellite Analysis Branch. The consensus of the Washington VAAC is that the TVAP provides improved monitoring of volcanic ash in many situations, and especially in the case of very weak eruptive activity. The technique is also being considered for use at the Montreal and Buenos Aires VAACs.

[42] The GOES TVAP is also generated hourly for selected areas, and made available on two Internet Web sites: (http://orbit-net.nesdis.noaa.gov/arad/fpdt/volc.html and http://www.ssd.noaa.gov/VAAC/table.html). The areas currently provided for these images are: (1) the eastern Caribbean (Soufriere Hills volcano), (2) southern Mexico (Popocatepetl and Colima), (3) Central America (numerous volcanoes), (4) Ecuador (Guagua Pichincha, Cotopaxi, Reventador, and Tungurahua) and (5) southern Alaska (numerous volcanoes). Evaluation by various users indicates that some false ash signatures can be seen, particularly from certain cirrus clouds (most likely newly-formed cirrus consisting of small ice particles) at low latitudes, but these situations can usually be diagnosed by a human analyst using pattern recognition techniques.

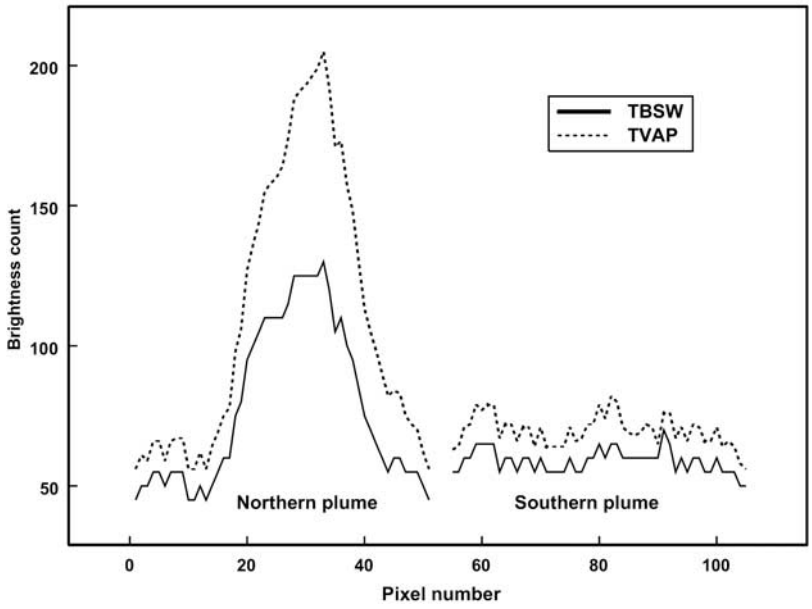


**Figure 12.** Trace of brightness count at each pixel across ash cloud at two locations (shown in Figure 8) for TBSW (solid line) and TVAP (dashed line) at 2245 UTC on 21 October 1997. One pixel equals 2 km distance at this scale. The locations of the northern and southern plume profiles are shown in the middle right panel of Figure 8.

[43] A future concern is that beginning with the GOES-12 spacecraft (successfully launched in July 2001 and activated on 1 April 2003), the "split window" (12.0 μm) band will not be provided again on the GOES Imagers until about 2013 when an Advanced Baseline Imager becomes available on GOES-R. The 12 μm IR band will therefore not be available to monitor volcanoes in North and South America, except for infrequent data from the lower resolution GOES sounder, or the NOAA or NASA polar-orbiters. Ash plumes from significant eruptions will still be observed in the IR data, but it will be more difficult to distinguish them from thin cirrus clouds, especially for long-lived eruption clouds. Additional research is needed to develop alternative strategies for optimum ash detection with the planned suite of IR bands that will include a new band centered near 13.3 μm. PCA has indicated that the latter band may contribute significantly toward volcanic ash detection by helping to discriminate volcanic ash from cirrus clouds [*Ellrod*, 2001] and may also contribute to more accurate estimation of ash cloud top heights.

## 8. Summary and Conclusions

[44] A technique for improved detection of volcanic ash has been developed that utilizes Brightness Temperature Differences (BTD) between three IR bands on GOES centered at 3.9, 10.7 and 12.0 μm wavelengths. The resulting BTDs are due to differences in radiative properties between silicate ash and surrounding meteorological clouds or underlying surfaces. Evaluation of the product shows improved ash detection in most cases, with the best results occurring during daytime, when there is strong solar reflectance in the 3.9 μm band, and at night over the ocean. There is also no significant over-enhancement of non-volcanic ash features when using the three-band technique. The method works well in cloudy regions, provided that the ash cloud is not completely obscured. Some false detection may occur during daylight in the vicinity of cirroform clouds. The three-band IR technique is under evaluation at the Washington Volcanic Ash Advisory Center, and is being considered for use at other VAACs.

## Notation

| | |
|---|---|
| B | brightness temperature, K. |
| C | constant. |
| $m_1$ | scale factor for two band split window infrared temperature difference. |
| $m_2$ | scale factor for shortwave minus longwave infrared temperature difference. |
| $T_2$ | infrared band 2 brightness temperature, K. |
| $T_4$ | infrared band 4 brightness temperature, K. |
| $T_5$ | infrared band 5 brightness temperature, K. |
| $\rho$ | reflectivity. |
| $\tau$ | transmissivity. |
| $\epsilon$ | emissivity. |
| μm | micrometer, $10^{-6}$ m. |

[45] **Acknowledgments.** The authors would like to thank the Washington Volcanic Ash Advisory Center (staffed by members of the Satellite Analysis Branch (NOAA/NESDIS)) for their willingness to evaluate the infrared satellite product described in this paper in their operations during the past 3 years.

## References

Ackerman, S. A., Using the radiative temperature difference at 3.7 and 11 μm to track dust outbreaks, *Remote Sens. Environ.*, *27*, 129–133, 1989.

Allen, R. C., P. A. Durkee, and C. H. Wash, Snow/cloud discrimination with multispectral satellite measurements, *J. Appl. Meteorol.*, *29*, 994–1004, 1990.

Arking, A., and J. D. Childs, Retrieval of cloud cover parameters from multispectral satellite images, *J. Clim. Appl. Meteorol.*, *24*, 322–333, 1985.

Bishop, K. D., J. A. Granger, and E. L. Jewett, Multispectral measurements of active lava flows by an airborne mid-wave infrared (MWIR) imaging spectrometer, paper presented at International Symposium on Spectral Sensing Research (ISSSR) '95, Int. Soc. for Photogramm. and Remote Sens., Melbourne, Australia, 1995.

Davies, M. A., and W. I. Rose, Evaluating GOES imagery for volcanic cloud observations at the Soufriere Hills volcano, Montserrat, *Eos Trans. AGU*, *79*, 505–507, 1998.

Dean, K., S. Bowling, G. Shaw, and H. Tanaka, Satellite analysis of movement and characteristics of the Redoubt Volcano plume, January 8, 1990, *J. Volcanol. Geotherm. Res.*, *62*, 339–352, 1994.

Ellrod, G. P., Advances in the detection and analysis of fog at night using GOES multispectral infrared imagery, *Weather Forecast.*, *10*, 606–619, 1994.

Ellrod, G. P., Loss of the 12 μm "split window" band on GOES-M: Impacts on volcanic ash detection, paper presented at 11th Conference on Satellite Meteorology and Oceanography, Am. Meteorol. Soc., Madison, Wisc., 15–18 Oct. 2001.

Hillger, D. W., GOES Imager and sounder calibration, scaling, and image quality, *NOAA Tech. Rep. NESDIS 93*, 34 pp., U.S. Dep. of Comm., Washington, D. C., 1999.

Hillger, D. W., and G. P. Ellrod, Detection of important atmospheric and surface features by employing principal component image transformation of GOES imagery, *J. Appl. Meteorol.*, *42*, 611–629, 2003.

Holasek, R. E., and W. I. Rose, Anatomy of 1986 Augustine volcano eruptions as revealed by digital AVHRR satellite imagery, *Bull. Volcanol.*, *53*, 420–435, 1991.

Hunt, G. E., Radiative properties of terrestrial clouds at visible and infrared thermal window wavelengths, *Q. J. R. Meteorol. Soc.*, *99*, 346–359, 1973.

Kidder, S. Q., and T. H. Vonder Haar, *Satellite Meteorology: An Introduction*, Academic, San Diego, Calif., 1995.

Kleespies, T. J., The retrieval of marine stratiform cloud properties from multiple observations in the 3.9 μm window under conditions of varying solar illumination, *J. Appl. Meteorol.*, *34*, 1512–1523, 1995.

Krotkov, N. A., A. J. Krueger, and P. K. Bhartia, Ultraviolet optical model of volcanic clouds for remote sensing of ash and sulfur dioxide, *J. Geophys. Res.*, *102*(D18), 21,891–21,904, 1997.

Lee, T. F., F. J. Turk, and K. Richardson, Stratus and fog products using GOES-8-9 3.9-μm data, *Weather Forecast.*, *12*, 664–677, 1997.

Mayberry, G. C., W. I. Rose, and G. J. S. Bluth, Dynamics of the volcanic and meteorological clouds produced by the December 26, 1997 eruption of Soufriere Hills volcano, Montserrat, WI, in *The Eruption of Soufriere Hills Volcano, Montserrat, From 1995 to 1999*, edited by T. Druitt, S. Young, and P. Kokelaar, *Geol. Soc. London Mem.*, *21*, 539–555, 2001.

Miller, T. P., and T. J. Casadevall, Volcanic ash hazards to aviation, in *Encyclopedia of Volcanoes*, edited by H. Sigurdsson, pp. 915–930, Academic, San Diego, Calif., 2000.

Oppenheimer, C., Volcanological applications of meteorological satellites, *Int. J. Remote Sens.*, *19*(15), 2829–2864, 1998.

Prata, A. J., Observations of volcanic ash clouds in the 10–12 micrometer window using AVHRR/2 data, *Int. J. Remote Sens.*, *10*, 751–761, 1989.

Prata, A. J., G. J. S. Bluth, W. I. Rose, D. J. Schneider, and A. Tupper, Comments on "Failures in detecting volcanic ash from a satellite-based technique", *Remote Sens. Environ.*, *78*, 341–346, 2001.

Rose, W. I., and G. C. Mayberry, Use of GOES thermal infrared imagery for eruption scale measurements, Soufriere Hills, Montserrat, *Geophys. Res. Lett.*, *27*, 3097–3100, 2000.

Rose, W. I., and D. J. Schneider, Satellite images offer aircraft protection from volcanic ash clouds, *Eos Trans. AGU*, *77*, 529, 532, 1996.

Salisbury, J. W., and L. S. Walter, Thermal infrared (2.5–13.5 um) spectroscopic remote sensing of igneous rock types on particulate planetary surfaces, *J. Geophys. Res.*, *94*(B7), 9192–9202, 1989.

Schneider, D. J., and W. I. Rose, Observations of the 1989–1990 Redoubt volcano eruption clouds using AVHRR satellite imagery, in *Volcanic Ash and Aviation Safety: Proceedings of the First International Symposium on Volcanic Ash and Aviation Safety*, *U.S. Geol. Surv. Bull*, *2047*, 405–418, 1994.

Schneider, D. J., W. I. Rose, and L. Kelley, Tracking of 1992 eruption clouds from Crater Peak/Spurr Volcano using AVHRR, *U.S. Geol. Surv. Bull.*, *2139*, 27–36, 1995.

Seftor, C. J., N. C. Hsu, J. R. Herman, P. K. Bhartia, O. Torres, W. I. Rose, D. J. Schneider, and N. Krotkov, Detection of volcanic ash clouds from Nimbus 7/Total Ozone Mapping Spectrometer, *J. Geophys. Res.*, *102*, 16,749–16,759, 1997.

Shannon, J. M., 3-D reconstruction of the Mt. Spurr volcanic clouds using AVHRR, TOMS and wind trajectory data, M.S. thesis, Mich. Tech. Univ., Houghton, 1996.

Simpson, J. J., G. Hufford, D. Pieri, and J. Berg, Failures in detecting volcanic ash from a satellite-based technique, *Remote Sens. Environ.*, *72*, 191–217, 2000.

Turk, J., J. Vivekanandan, T. Lee, P. Durkee, and K. Nielsen, Derivation and applications of near-infrared cloud reflectances from GOES-8 and GOES-9, *J. Appl. Meteorol.*, *37*, 819–831, 1998.

Vickers, R. S., and R. P. Lyon, Infrared sensing from spacecraft: A geological interpretation, in *Thermophysics of Spacecraft and Planetary Bodies: Radiation Properties of Solids and the Electromagnetic Radiation Environment in Space*, edited by G. B. Heller, pp. 585–607, Academic, San Diego, Calif., 1967.

Volz, F. E., Infrared optical constants of ammonium sulfate, Sahara dust, volcanic pumice and flyash, *Appl. Opt.*, *12*, 564–568, 1973.

Watkin, S., M. Ringer, and A. Baran, Investigation into the use of SEVIRI imagery for the automatic detection of volcanic ash clouds, paper presented at 2000 EUMETSAT Meteorological Satellite Data Users Conference, Bologna, Italy, 24 May to 4 June 2000.

Yu, T., W. I. Rose, and A. J. Prata, Atmospheric correction for satellite based volcanic ash mapping and retrievals using "split window" IR data from GOES and AVHRR, *J. Geophys. Res.*, *107*(D16), 4311, doi:10.1029/2001JD000706, 2002.

B. H. Connell, Cooperative Institute for Research in the Atmosphere, Foothills Campus, Colorado State University, Fort Collins, CO 80523-1375, USA.

G. P. Ellrod, Office of Research and Applications, NOAA/NESDIS, 5200 Auth Road, Room 601, E/RA2, Camp Springs, MD 20746, USA. (gary.ellrod@noaa.gov)

D. W. Hillger, Regional and Mesoscale Meteorology Team, NOAA/NESDIS, Foothills Campus, Colorado State University, Fort Collins, CO 80523-1375, USA.